Low-temperature magnetic phase diagram of $HoFe_3(BO_3)_4$ holmium ferroborate: a magnetic and heat capacity study

2009 J. Phys.: Condens. Matter 21 436001

(http://iopscience.iop.org/0953-8984/21/43/436001)

J. Phys.: Condens. Matter **21** (2009) 436001 (5pp) doi:10.1088/0953-8984/21/43/436001

Low-temperature magnetic phase diagram of $HoFe_3(BO_3)_4$ holmium ferroborate: a magnetic and heat capacity study

A Pankrats[1], G Petrakovskii[1,2], A Kartashev[1], E Eremin[1] and V Temerov[1]

[1] Kirensky Institute of Physics, SB RAS, 660036 Krasnoyarsk, Russia
[2] Department of Physics, Siberian Federal University, 660041 Krasnoyarsk, Russia

E-mail: pank@iph.krasn.ru

Received 3 June 2009, in final form 6 August 2009
Published 5 October 2009
Online at stacks.iop.org/JPhysCM/21/436001

Abstract

We present the results of the magnetic and heat capacity study of a magnetic phase diagram of a $HoFe_3(BO_3)_4$ single crystal. Two magnetic phase transitions are found in the low-temperature region. The transition from the paramagnetic to easy-plane antiferromagnetic state occurs at $T_N = 37.4$ K and is independent of an applied magnetic field. The sharp heat capacity peaks and magnetization jumps corresponding to the spontaneous and field-induced spin-reorientation transitions between the easy-axis and easy-plane states are observed below 4.7 K. Also, the additional heat capacity peaks, which can be attributed to the Schottky anomalies with the field-dependent characteristic temperatures, are found. According to the magnetic and thermal measurement data, the magnetic phase diagrams of $HoFe_3(BO_3)_4$ for the magnetic field parallel and perpendicular to the crystal axis are constructed.

1. Introduction

The family of rare-earth ferroborates with the general formula $RA_3(BO_3)_4$ and *huntite* structure where R^{3+} is a rare-earth or Y^{3+} ion and A = Al, Ga, Sc, Cr or Fe have drawn the attention of researchers primarily as a medium for nonlinear optics and laser techniques [1–3]. However, the coexistence of two magnetic subsystems of iron and rare-earth ions coupled by the exchange interaction in $RFe_3(BO_3)_4$ causes the interesting magnetic properties of this family of crystals. The competition of magnetic anisotropies of these subsystems provides a rich variety of magnetic structures for the crystals with different rare-earth ions. The AFMR investigation [4] and neutron study of the magnetic structure [5] showed that, in the case of nonmagnetic Y^{3+} ions, the magnetic properties of the crystal are determined only by the iron subsystem, which represents an easy-plane (EP) antiferromagnet with the Néel temperature $T_N = 38$ K and magnetic moments lying in the basal plane. In $NdFe_3(BO_3)_4$, the magnetic anisotropy of Nd^{3+} ions stabilizes the EP magnetic structure with $T_N = 30.5$ K and, in accordance with the neutron data [6], below 19 K the incommensurate spiral magnetic configuration with the magnetic moments parallel to the basal plane occurs. In the crystals with R = Tb [7, 8], Dy [9, 10] and Pr [11], the easy-axis (EA) magnetic structure is established due to the prevailing magnetic anisotropy of these rare-earth ions. In gadolinium ferroborate $GdFe_3(BO_3)_4$ where, as follows from the AFMR data [4, 12], the contributions of the rare-earth and iron subsystems have the opposite signs and are close to the absolute value, the difference between the temperature dependences of the contributions induces the spontaneous spin-reorientation transition between the EA and EP states with $T_{SR} = 10$ K. The temperature of the transition depends on the strength and orientation of the magnetic field. Using the AFMR data [12] and the results of the magnetic [13] and magnetostrictive measurements [14], the magnetic phase diagrams of this crystal were constructed for the magnetic fields oriented along the crystal axis and in the basal plane.

The common property of all the $RFe_3(BO_3)_4$ crystals is that the exchange interaction in the rare-earth subsystem is weak; however, due to the exchange interaction with Fe^{3+} ions, the magnetic order in both subsystems occurs simultaneously.

Some crystals of this family with R = Gd, Nd and Pr reveal the multiferroic properties [11, 14, 15] but the magnetoelectric effect is found only in those crystals with certain magnetic structures. This fact also stimulates interest

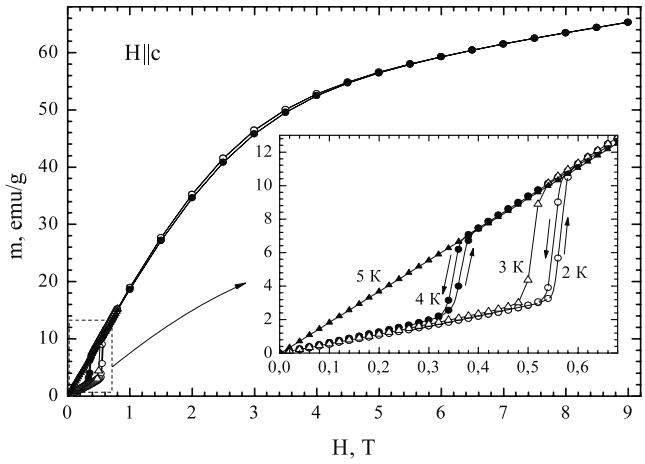

Figure 1. Magnetic field dependences of $HoFe_3(BO_3)_4$ magnetization measured along the crystal axis at different temperatures. Inset: $M(H)$ dependence enlarged over the low-temperature range.

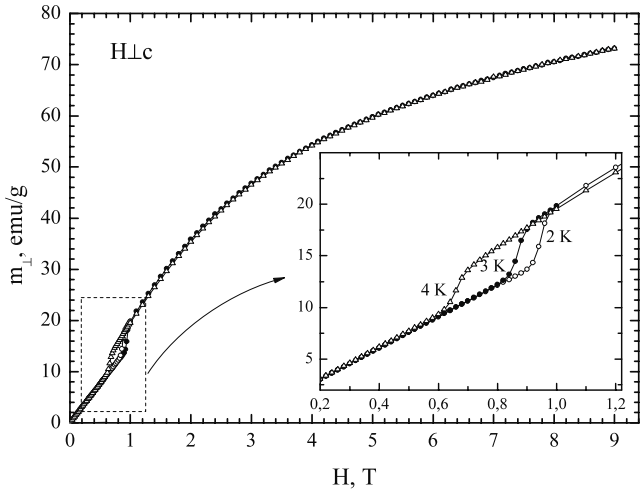

Figure 2. The magnetic field dependences of magnetization of $HoFe_3(BO_3)_4$ measured in the basal plane at various temperatures. Inset: $M(H)$ dependence enlarged in the low-temperature range.

in the dependence of the magnetic properties of the crystals on the rare-earth ions.

The magnetic structure of $HoFe_3(^{11}BO_3)_4$ similar to that of $GdFe_3(BO_3)_4$ was established by neutron scattering in our previous work [5]. In particular, the spontaneous phase transition between the high-temperature EP and low-temperature EA magnetic phases was found to occur at $T_{SR} \approx 5$ K. In the mentioned study, the preliminary magnetic measurement data confirming the results of the neutron measurements were also reported. The obtained data allowed us to assume that, at temperatures below T_{SR}, the crystal can be transferred from the EA state to the EP state which is induced by magnetic field.

In the present study, we consider in detail the low-temperature magnetic phase diagram of $HoFe_3(BO_3)_4$. According to the data of magnetic measurements, the temperatures of the spin-reorientation transitions between the EA and EP states decrease with an increase in magnetic field applied both along the trigonal axis and in the basal plane. Sharp heat capacity anomalies corresponding to the spontaneous phase transition at $T_{SR} = 4.7$ K in zero magnetic field and to the magnetic-field-induced phase transitions are found. On the basis of the heat capacity and magnetic data, the magnetic phase diagrams of $HoFe_3(BO_3)_4$ for both orientations of the magnetic field are constructed.

2. Samples and experimental methods

$HoFe_3(BO_3)_4$ single crystals up to $5 \times 5 \times 5$ mm^3 in size were grown using a $Bi_2Mo_3O_{12}$-based flux [16]. The same process of synthesizing was applied for crystals used in neutron experiments [5]. The single crystals had pronounced grown edges, one of which had a regular triangular shape and was perpendicular to the crystallographic threefold axis. For the measurements, samples about $2 \times 2 \times 2$ mm^3 in size were cut.

The magnetic and thermal properties were investigated with a Quantum Design Physical Properties Measurement System (PPMS 6000) in magnetic fields up to 9 T at temperatures down to 1.9 K. For the preliminary study of magnetic resonance in $HoFe_3(BO_3)_4$, a computer-controlled magnetic resonance spectrometer with a pulsed magnetic field was used.

3. Experimental results

The temperature dependences of magnetic susceptibility of the $HoFe_3(BO_3)_4$ single crystal for the magnetic fields $H \parallel c$ and $H \perp c$ coincide with our SQUID magnetometer data reported in [5]. The measured values of magnetic susceptibility are caused by the contributions of the magnetic subsystems of iron and holmium ions; the values of paramagnetic temperatures $\theta_\parallel$ and $\theta_\perp$ averaged over both subsystems and effective magnetic moments $\mu_\parallel$ and $\mu_\perp$ are close to those measured in [5].

The field dependences of magnetization $m_\parallel$ measured along the crystal axis are depicted in figure 1. The inset shows the portions of the dependences enlarged over the field range near the spin-reorientation transition for several temperatures. The magnetization jumps are related to reorientation of the magnetic structure from the EA to EP state and are determined by the difference between magnetic susceptibilities $\chi_\parallel$ and $\chi_\perp$ in the appropriate states. The critical field of the phase transition decreases as the temperature increases and approaches the spontaneous reorientation temperature; at $T = 5$ K the transition is not observed. Small magnetic hysteresis which is found to occur upon spin reorientation at 2 and 4 K suggests the first-order character of the phase transition (the hysteresis was not studied at 3 K).

The magnetization in the basal plane behaves similarly (figure 2). The $m_\perp$ jumps observed at temperatures below 5 K also correspond to spin reorientation between the EA and EP states. At such orientations of the magnetic field, magnetization is determined by perpendicular susceptibility in both states. The minor difference between the EA and EP susceptibilities caused by uniaxial magnetic anisotropy yields

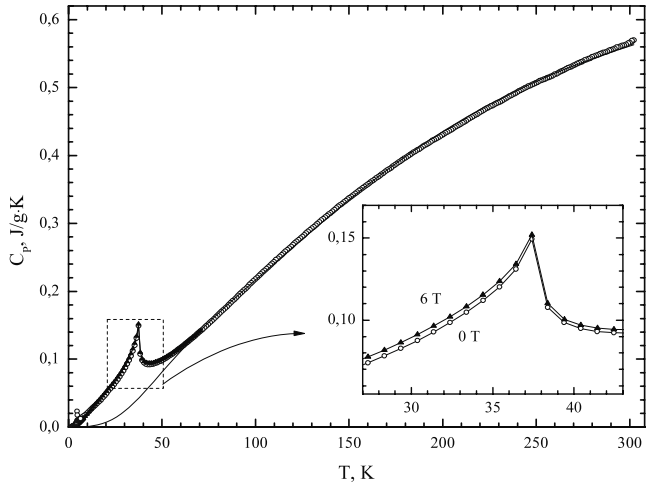

Figure 3. Temperature dependence of heat capacity taken in zero magnetic field and in a field of 6 T along the crystal axis. Inset: the portion of the dependence near the Néel temperature.

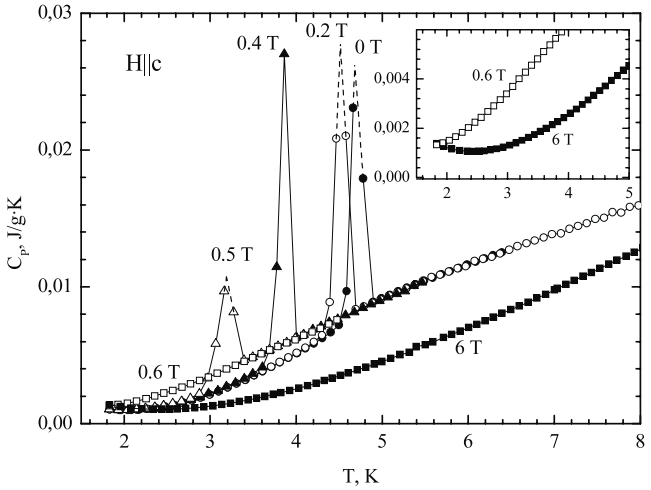

Figure 4. Low-temperature portion of heat capacity measured in different magnetic fields applied along the crystal axis.

a small magnetization jump during the phase transition. The critical fields are higher than those at parallel orientation of the field for the same temperatures and also decrease as the temperature of the spontaneous transition is approached.

The phase transitions were studied also by thermal measurements. The temperature dependences of heat capacity measured in zero magnetic field and in an external magnetic field of 6 T applied along the crystal axis are presented in figure 3. The heat capacity peak of a typical λ form at $T = 37.4$ K is related to the onset of the long-range magnetic order in the crystal and corresponds to the Néel temperature of the iron subsystem. Such a value of T_N coincides with that found in neutron scattering measurements [5]. The phonon contribution to heat capacity calculated using the Debye model with $\theta_D = 290$ K is shown by the solid line in the figure. From comparison with the experimental data one can see that the magnetic fluctuations due to the occurrence of the magnetic order begin at $T \approx 60$ K and are built up as the Néel temperature is approached. The inset shows the enlarged area of the magnetic phase transition. No shift of this peak in an external magnetic field of 6 T is observed in $HoFe_3(BO_3)_4$ as well as in the related $NdFe_3(BO_3)_4$ crystal [6], in contrast to $TbFe_3(BO_3)_4$ [8], where the Néel temperature exhibits an appreciable dependence on applied magnetic field.

The temperature dependence of heat capacity presented in figure 3 differs from that measured for polycrystalline $HoFe_3(BO_3)_4$ in [17] by the presence of an additional sharp low-temperature peak with a width of about 0.5 K. The low-temperature portions of $HoFe_3(BO_3)_4$ heat capacity measured without a magnetic field and in the external field applied along the crystal axis are shown in figure 4. The sharp peaks correspond to the spin-reorientation phase transitions between the EA and EP states. This peak was missed in [17] apparently because of the temperature step exceeding the width of the peak. The spontaneous transition in zero magnetic field occurs at the temperature $T_{SP} = 4.7$ K. Similar to the results of the magnetic measurements, the temperature of the phase transition decreases with an increase in magnetic field.

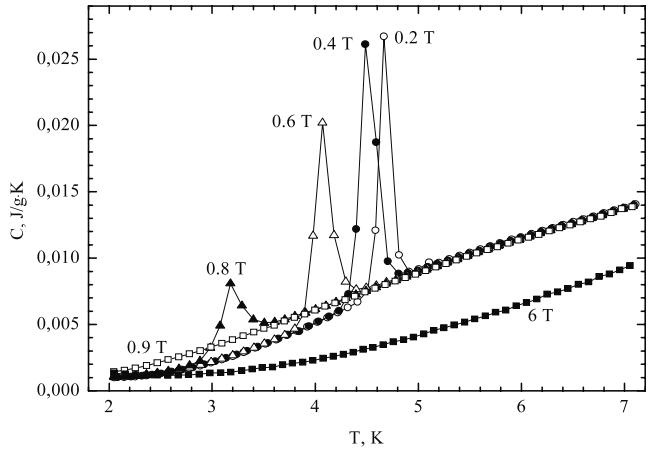

Figure 5. Low-temperature portion of heat capacity measured in different magnetic fields applied in the crystal basal plane.

The temperature dependences of heat capacity measured in a magnetic field lying in the basal plane are similar; their low-temperature portions are shown in figure 5. The sharp peaks of heat capacity are observed upon spin reorientations; critical temperatures of transitions decrease with an increase in magnetic field.

4. Discussion

The spin-reorientation phase transition between the low-temperature EA and high-temperature EP states in both $HoFe_3(BO_3)_4$ and gadolinium ferroborate $GdFe_3(BO_3)_4$ originates from the competition of the contributions of the iron and rare-earth subsystems to the total magnetic anisotropy of the crystal. The magnetic anisotropy of the iron subsystem stabilizes the EP magnetic structure [4]. The contribution to the total anisotropy made by the holmium subsystem obviously has the opposite sign which corresponds to the EA structure. The close absolute values of both contributions

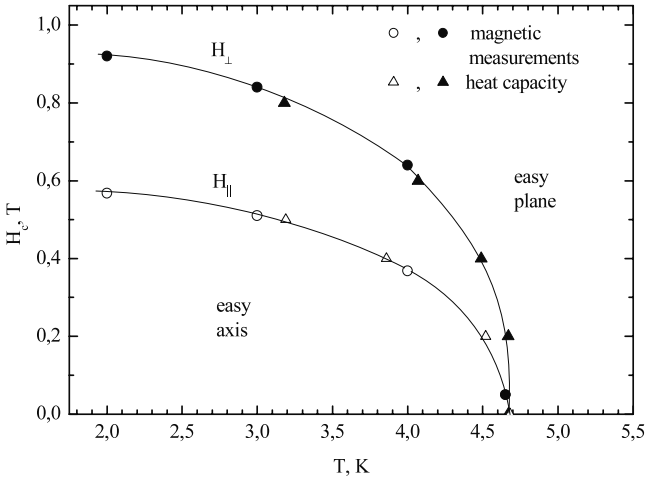

Figure 6. Magnetic phase diagrams for $HoFe_3(BO_3)_4$ in magnetic fields applied parallel and perpendicular to the crystal axis.

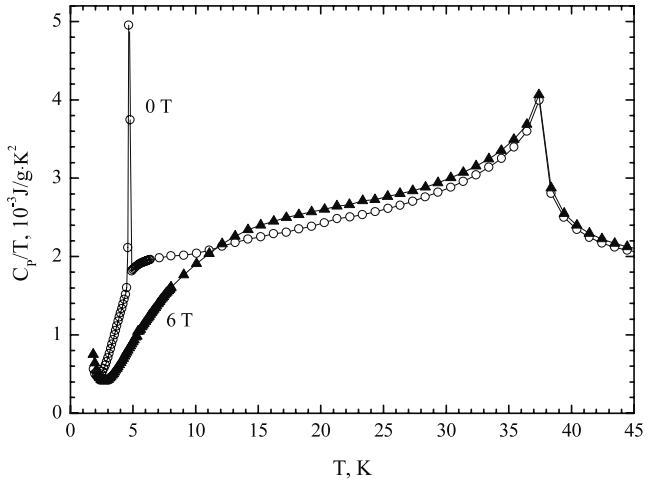

Figure 7. Temperature dependence of parameter C_p/T taken in zero magnetic field and in a field of 6 T along the crystal axis.

and their different temperature dependences result in the spin-reorientation transition.

As for the ratio of magnetic anisotropies of Gd^{3+} and Ho^{3+} ions, the preliminary AFMR[3] study of the $HoFe_3(BO_3)_4$ single crystal shows that the energy gap in the EA state spectrum at $T = 4.2$ K is $\nu_c \approx 80$ GHz. Since the magnetic anisotropy of the iron subsystem does not change, the increase in the energy gap as compared to gadolinium ferroborate ($\nu_c = 29.4$ GHz) is caused by the fact that the magnetic anisotropy of Ho^{3+} ions exceeds that of Gd^{3+} ions. At the same time, the temperature of $HoFe_3(BO_3)_4$ spontaneous reorientation $T_{SP} = 4.7$ K at which the total anisotropy of the crystal changes its sign is considerably lower compared to $T_{SP} = 10$ K for $GdFe_3(BO_3)_4$. It implies that the temperature dependence of the anisotropy field for Ho^{3+} ions at low temperatures is stronger than that for Gd^{3+}.

Since the contributions of both subsystems to the total anisotropy of $HoFe_3(BO_3)_4$ compensate substantially each other, the magnetic structure appears very sensitive to the effect of the external magnetic field, temperature and doping by other rare-earth ions. In particular, spectroscopic studies of $HoFe_3(BO_3)_4$ were performed using an Er^{3+} ion as a probe. The spin-reorientation transition is not observed in the crystal doped by 1% of Er^{3+} with the EP anisotropy, at least down to the temperature $T = 4.2$ K [18].

The temperature dependences of the critical fields of the transitions between the EA and EP states in $HoFe_3(BO_3)_4$ for both orientations of the magnetic field are plotted using the data of magnetic and thermal measurements. Figure 6 showing these dependences presents the $HoFe_3(BO_3)_4$ magnetic phase diagrams in the corresponding magnetic fields. The EA and EP states are arranged under and outside the appropriate phase boundary, respectively.

Now let us pass to the discussion of heat capacity. The temperature dependences of parameter C_p/T (see figure 7) exhibit wide heat capacity peaks at temperatures of 5 and 15 K in zero magnetic field and at 6 T, respectively. In addition, on approaching the temperature 1.9 K heat capacity measured in a magnetic field of 6 T starts increasing sharply, testifying to the existence of one more heat capacity peak at lower temperature. This feature is observed for both orientations of the magnetic field and is clearly seen in the inset of figure 4. Most likely, such a behavior can be attributed to the Schottky anomalies depending on the applied magnetic field. The similar field dependence of the Schottky anomaly was observed in $TbFe_3(BO_3)_4$ [8]. Apparently, the existence of several Schottky anomalies in $HoFe_3(BO_3)_4$ points to the specific structure of Ho^{3+} ion energy levels containing a set of relatively low-lying levels [19]. Indeed, the optical spectroscopic study of $HoFe_3(BO_3)_4$ at $T = 50$ K reveals a set of low-lying Ho^{3+} singlets at 0, 8.5, 14.1, 18.3, etc cm^{-1} [20]. It is obvious that the positions of the energy levels change under the applied magnetic field, which results in the field-dependent characteristic temperatures of anomalies. In addition, below the Néel temperature the molecular field from the Fe^{3+} subsystem is added to the external magnetic field.

Figure 7 shows that the wide heat capacity peak observed in the area of the spin-reorientation transition in zero magnetic field looks much sharper as compared to the Schottky anomaly at 15 K in a field of 6 T. Seemingly, in this case, the Schottky anomaly and the additional heat capacity peak related to spin reorientation are superimposed on one another. Upon cooling the sample below the transition, heat capacity drops much faster than it does above the transition. As follows from figures 4 and 5, this feature is observed not only in zero magnetic field but also in relatively small fields in the area of the phase transition. As a result, the heat capacity values measured at the same temperature in different magnetic fields and, hence, in different magnetic states are substantially different. Heat capacity of the EA state appears lower than that of the EP state at the same temperature. It implies that the degree of the low-temperature EA state ordering is higher as compared to the EP state. It can be explained by the fact that, in accordance with the neutron data [5], the magnetic

[3] The AFMR experimental data for $HoFe_3(BO_3)_4$ will be published elsewhere.

structure of the Fe^{3+} subsystem, which is mainly responsible for the magnetic order of the crystal, is collinear and weak noncollinear in the EA and EP states, respectively.

The additional wide heat capacity peak related to the spin-reorientation transition remains even in the applied magnetic fields which are above the phase boundary but rather close to it. In particular, as is seen in figures 4 and 5, the wide peaks are present in magnetic fields of 0.6 and 0.9 T applied along the crystal axis and in the basal plane, respectively.

5. Conclusions

The magnetic and thermal studies confirm the existence of the two low-temperature magnetic phase transitions in $HoFe_3(BO_3)_4$, specifically the transition from the paramagnetic to EP antiferromagnetic state at $T_N = 37.4$ K and spontaneous spin reorientation to the EA state at $T_{SR} = 4.7$ K, which is explained by the competition of the magnetic anisotropies of the iron and holmium subsystems with the opposite signs. The magnetic resonance data suggest the strong temperature dependence of the holmium contribution to the total magnetic anisotropy.

The Néel temperature T_N of $HoFe_3(BO_3)_4$ is found to be independent of the applied magnetic field. The low-temperature data on heat capacity exhibit broad peaks due to the Schottky anomalies with the critical temperatures depending on the applied magnetic field and the narrow (about 0.5 K) peaks corresponding to the spin-reorientation transition.

The phase transitions from the EA to field-induced EP state are found below T_{SR} in external magnetic fields $H \parallel c$ and $H \perp c$; the critical temperatures of the phase transitions decrease with an increase in magnetic field. The magnetic phase diagrams of $HoFe_3(BO_3)_4$ are constructed for both orientations of magnetic field.

Acknowledgments

We are grateful to M Popova and E Chukalina for data on the energy structure of the Ho^{3+} ion in $HoFe_3(BO_3)_4$ kindly placed at our disposal before they are published. We thank also V Tugarinov for preliminary data on magnetic resonance in the crystal.

References

[1] Chani V I, Timoshechkin M I, Inoue K, Shimamura K and Fukuda T 1994 *Inorg. Mater.* **30** 1466
[2] Huang M *et al* 2002 *Opt. Commun.* **208** 163
[3] Chen X, Luo Z, Romero J J, Sole J G, Huang Y, Jiang A and Tu Ch 2001 *J. Phys.: Condens. Matter* **13** 1171
[4] Pankrats A, Petrakovski G, Bezmaternykh L and Temerov V 2008 *Phys. Solid State* **50** 79
[5] Ritter C, Vorotynov A, Pankrats A, Petrakovskii G, Temerov V, Gudim I and Szymczak R 2008 *J. Phys.: Condens. Matter* **20** 365209
[6] Fischer P, Pomjakushin V, Sheptyakov D, Keller L, Janoschek M, Roessli B, Schefer J, Petrakovskii G, Bezmaternikh L, Temerov V and Velikanov D 2006 *J. Phys.: Condens. Matter* **18** 7975
[7] Ritter C, Balaev A, Vorotynov A, Petrakovskii G, Velikanov D, Temerov V and Gudim I 2007 *J. Phys.: Condens. Matter* **19** 196227
[8] Popova E A, Volkov D V, Vasiliev A N, Demidov A A, Kolmakova N P, Gudim I A and Bezmaternykh L N 2007 *Phys. Rev.* **B 75** 224413
[9] Gudim I A, Pankrats A I, Durnaykin E I, Petrakovskii G A, Bezmaternykh L N, Szymczak R and Baran M 2008 *Crystallogr. Rep.* **53** 1140
[10] Popova E A, Tristan N, Vasiliev A N, Temerov V L, Bezmaternykh L N, Leps N, Buchner B and Klingeler R 2008 *Eur. Phys. J.* B **62** 123
[11] Kadomtseva A M, Popov Yu F, Vorob'ev G P, Mukhin A A, Ivanov V Yu, Kuz'menko A M and Bezmaternykh L N 2008 *JETP Lett.* **87** 39
[12] Pankrats A I, Petrakovskii G A, Bezmaternykh L N and Bayukov O A 2004 *JETP* **99** 766
[13] Kharlamova S A, Ovchinnikov S G, Balaev A D, Thomas M F, Lyubutin I S and Gavriliuk A G 2005 *JETP* **101** 1098
[14] Zvezdin A K, Krotov S S, Kadomtseva A M, Vorob'ev G P, Popov Yu F, Pyatakov A P, Bezmaternykh L N and Popova E A 2005 *JETP Lett.* **81** 272
[15] Zvezdin A K, Vorob'ev G P, Kadomtseva A M, Popov Yu F, Pyatakov A P, Bezmaternykh L N, Kuvardin A V and Popova E A 2006 *JETP Lett.* **83** 509
[16] Bezmaternykh L N, Temerov V L, Gudim I A and Stolbovaya N A 2005 *Crystallogr. Rep.* **50** 97
[17] Hinatsu Y, Doi Y, Ito K, Wakeshima M and Alemi A 2003 *J. Solid State Chem.* **172** 438
[18] Stanislavchuk T N, Chukalina E P, Popova M N, Bezmaternykh L N and Gudim I A 2007 *Phys. Lett.* A **368** 408
[19] Zvezdin A K, Matveev V M, Mukhin A A and Popov A I 1985 *Rare-Earth Ions in Magnetic Ordered Crystals* (Moscow: Nauka) p 296
[20] Popova M N and Chukalina E P, private communication